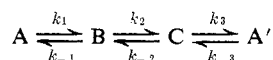


nmr integral measurements were performed using a Varian HA-100 instrument operating at 30°. The samples of **1** were kept in the probe throughout the reaction except for the determination of the exchange rates of H<sub>1</sub> vs. H<sub>4</sub> in CD<sub>3</sub>OD. For these measurements the sample was kept in a constant-temperature bath at 60°, except for periodic determination of integrals. In the exchange reaction of **2**, a sample (50 mg) was dissolved in 0.5 ml of CD<sub>3</sub>OD containing CD<sub>3</sub>ONa (0.3 M) in a heavy-walled Pyrex tube. The tube was sealed and heated for 72 hr at 120°, cooled, and opened. The solvent was distilled off and the residue was sublimed to give a pure sample of **2** whose nmr spectrum showed that 58.5% exchange had occurred in the exo position while no endo exchange was detectable (<0.75%). Under similar conditions (110°, 48 hr in CD<sub>3</sub>OD containing CD<sub>3</sub>ONa (0.5 M)) an exchanged sample of **3** showed that 35% exchange in the endo position and 11% exchange in the exo position had occurred. The nmr spectra of **2** and **3** were measured during simultaneous irradiation of the deuterium atoms with an NMR Specialties SD-100 deuterium spin-decoupler.

## Appendix

For a detailed consideration of the rate processes depicted in Figure 3, we can use the following scheme



in which A and A' represent the same initial substrate. H-D exchange *via* the step designated by  $k_3$  will produce monodeuterated A' which is a diastereomer of monodeuterated A resulting from the step designated by  $k_{-1}$ .

The differential equations for time-dependent behavior of intermediates B and C are

$$d[B]/dt = k_1[A] + k_{-2}[C] - k_{-1}[B] - k_2[B]$$

$$d[C]/dt = k_{-3}[A] + k_2[B] - k_3[C] - k_{-2}[C]$$

Since B and C are interconverted *via* the carbanion inversion barrier,  $k_2[B] = k_{-2}[C]$

$$d[B]/dt = k_1[A] - k_{-1}[B]$$

$$d[C]/dt = k_{-3}[A] - k_3[C]$$

Also, assuming the steady-state equilibrium, then  $d[B]/dt = d[C]/dt = 0$  and  $k_{-1}[B] = k_1[A]$  and  $k_3[C] = k_{-3}[A]$ . Now

$$\frac{\text{rate of formation of A}}{\text{rate of formation of A}'} = \frac{k_{-1}[B]}{k_3[C]} = \frac{k_1}{k_{-3}}$$

*i.e.*, since  $k_1$  and  $k_{-3}$  involve the same ground states, the difference in the rates of formation of the deuterated species A and A' is governed solely by the difference in the transition states B<sup>‡</sup> and C<sup>‡</sup>.

**Acknowledgments.** The authors thank the National Research Council of Canada for generous financial support. Discussions of many aspects of this work with Professors D. J. Cram, T. Durst, and S. Wolfe have proven very valuable.

## Conformational Dependence of the Electronic Energy Levels in Disulfides

Donald B. Boyd

*Contribution from The Lilly Research Laboratories, Eli Lilly and Company, Indianapolis, Indiana 46206. Received February 28, 1972*

**Abstract:** The energies of extended Hückel molecular orbitals of model disulfides are studied as a function of dihedral angle about the S-S bond. Transition energies and oscillator strengths obtained in the virtual orbital approximation, but with exactly evaluated transition moment integrals, satisfactorily match experimental trends. Although the S 3d atomic orbitals are not highly occupied in the ground states of HSSH and H<sub>3</sub>CSSCH<sub>3</sub>, the inclusion of these orbitals in the basis set increases the number of low-lying excited states appropriate for uv absorption. The lowest energy transition of the disulfide chromophore involves an S-S σ\* virtual MO and lone-pair occupied MO's. Because of the conformational dependence of the latter MO's, the lowest energy transition red-shifts and loses intensity as the dihedral angle is twisted from 90 toward 0 or 180°. An explanation of the spectra of bulky dialkyl disulfides is based on the very weak intensity predicted for the lowest energy transition when the dihedral angle is opened beyond 90°. Calculated barriers to internal rotation are in fair agreement with microwave data on HSSH and H<sub>3</sub>CSSCH<sub>3</sub>. Insight into the origin of the rotational barrier is provided by population analyses, which show a repulsive interaction of the lone-pair electrons.

The conformation of a disulfide bridge in proteins and other biomolecules can often be deduced from the uv and CD spectra of these molecules. Molecules of known conformation and absolute configuration have been studied spectroscopically, and a correlation has been found between the energy of the lowest energy uv transition and the dihedral angle about the S-S bond. This correlation is exemplified by the data in Table I taken from the literature.<sup>1-8</sup> As the CSSC

dihedral angle is opened from 0 to 90°, the absorption maximum of the first uv band shifts from near 370 to

(4) M. Calvin and J. A. Barltrop, *ibid.*, 74, 6153 (1952); A. F. Beecham, J. W. Loder, and G. B. Russell, *Tetrahedron Lett.*, 1785 (1968).

(5) M. Carmack and L. A. Neubert, *J. Amer. Chem. Soc.*, 89, 7134 (1967); G. Claesson, *Acta Chem. Scand.*, 22, 2429 (1968); O. Foss, K. Johnsen, and T. Reistad, *ibid.*, 18, 2345 (1964); L. A. Neubert, Ph.D. Thesis, Indiana University, Bloomington, Ind., 1969.

(6) S. D. Thompson, D. G. Carroll, F. Watson, M. O'Donnell, and S. P. McGlynn, *J. Chem. Phys.*, 45, 1367 (1966). It is not clear from this paper that the rotationally invariant form of Cusachs' EH method was employed. The original Cusachs' version produced eigenvalues dependent on the coordinate system selected for the molecule; see M. D. Newton, *ibid.*, 45, 2716 (1966).

(7) G. M. Bogolyubov and Y. N. Shlyk, *J. Gen. Chem. USSR*, 39, 1723 (1969).

(8) U. Ludescher and R. Schwyzer, *Helv. Chim. Acta*, 54, 1637 (1971).

(1) G. Bergson, G. Claesson, and L. Schotte, *Acta Chem. Scand.*, 16, 1159 (1962).

(2) A. F. Beecham and A. McL. Mathieson, *Tetrahedron Lett.*, 3139 (1966).

(3) R. Nagarajan, N. Neuss, and M. M. Marsh, *J. Amer. Chem. Soc.*, 90, 6518 (1968); D. B. Cosulich, N. R. Nelson, and J. H. van den Hende, *ibid.*, 90, 6519 (1968).

**Table I.** Observed Variation of the Longest Wavelength Transition with Dihedral Angle in Disulfides

Compound	Dihedral angle, deg	$\lambda_{\max}$ , nm	$\epsilon_{\max}$	Ref
1 $\alpha$ ,5 $\alpha$ -Epidithioandrostandi- 3 $\alpha$ ,17 $\beta$ -diol	~0	370	50	1
Gliotoxin	9-16	340	200	2
Acetylaranotin	15-18	345		3
6,8-Thioctic acid	~30	330	180	1, 4
1,2-Dithianes	~60	280-290	300-400	5
Dimethyl disulfide	85	250-255	330-520	6, 7
[2,7-Cystine]-gramicidin S	~120	272		8

about 250 nm, and the extinction coefficient increases several fold. Recent evidence<sup>8</sup> shows that when the dihedral angle is increased beyond 90 to about 120°, the transition shifts back toward the red.

The main purpose of this paper is to understand these trends from molecular orbitals (MO's) calculated by the semiempirical extended Hückel (EH) method.<sup>9</sup> The utility of EH theory in spectral correlations and assignments is occasionally maligned, but recent studies<sup>10,11</sup> have shown it to be very useful on at least a qualitative basis. Several semiempirical quantum mechanical studies<sup>6,12-14</sup> on the disulfide chromophore have appeared in the literature, but various limitations of the earlier work make further calculations worthwhile. In our calculations, hydrogen persulfide, HSSH, and dimethyl disulfide, H<sub>3</sub>CSSCH<sub>3</sub>, will be assigned dihedral angles through the whole range of interesting values from 0° to 180°, as well as the experimental values near 90°. Thereby the relationship of dihedral angle and uv absorption spectra can be modeled for investigation. A full basis set of valence atomic orbitals (AO's) is employed, including the 3d orbitals of sulfur. Whereas one may expect the 3d's to be of only minor consequence on the filled MO's, they play a large role in determining the low-lying excited states.<sup>10</sup> Hence the parameters for the 3d AO's were carefully selected to provide a reasonable overall description of charge distributions, dipole moments, and excitation energies of other divalent sulfur compounds, such as dimethyl sulfide, 3-cephem, and penam. The uv spectra of the latter two compounds, which are important moieties in  $\beta$ -lactam antibiotics, have been interpreted by EH calculations elsewhere.<sup>10</sup> As will be seen later, numerical agreement with experimental transition energies is especially good in disulfides with dihedral angles near 90°. This would indicate that our parameters have some general applicability to sulfides without empirical adjustments for each different compound. Also with our parameters, the total occupation of the 3d AO's in ground state HSSH turns out to be almost the same (~0.1 electron) as recently obtained in large basis set *ab initio* calculations (*vide infra*). A final aspect of our calculations on the di-

(9) D. B. Boyd and W. N. Lipscomb, *J. Theor. Biol.*, **25**, 403 (1969); R. Hoffmann, D. B. Boyd, and S. Z. Goldberg, *J. Amer. Chem. Soc.*, **92**, 3929 (1970).

(10) D. B. Boyd, *ibid.*, **94**, 6513 (1972).

(11) D. L. Coffen, J. Q. Chambers, D. R. Williams, P. E. Garrett, and N. D. Canfield, *ibid.*, **93**, 2258 (1971); L. Burnelle and M. J. Kranspool, *J. Mol. Spectrosc.*, **37**, 383 (1971).

(12) G. Bergson, *Ark. Kemi*, **12**, 233 (1958); **18**, 409 (1962).

(13) J. Linderberg and J. Michl, *J. Amer. Chem. Soc.*, **92**, 2619 (1970).

(14) H. Yamabe, H. Kato, and T. Yonezawa, *Bull. Chem. Soc. Jap.*, **44**, 604 (1971).

sulfide chromophore is that transition dipole integrals are rigorously evaluated. All one- and two-center integrals over the Slater-type orbitals are computed.<sup>15</sup> In contrast, earlier studies have usually employed zero differential overlap (ZDO) approximations. Later in our paper, results from the earlier studies will be compared to our findings.

### Computational Details

Microwave analyses of HSSH<sup>16</sup> and H<sub>3</sub>CSSCH<sub>3</sub><sup>17</sup> provided the nuclear geometries needed for the EH calculations. Bond lengths and angles were held fixed as the dihedral angle about the S-S bond was varied from 0 to 180° in 30° intervals. Hamiltonian matrix elements were constructed from previously published formulae and parameters.<sup>9,10</sup> The quantity  $\frac{1}{2}\Sigma\epsilon_i$  is used for computing rotational barriers. Here the eigenvalues,  $\epsilon_i$ , of each occupied MO are summed over all valence electrons. It has been shown that this quantity (rather than  $\Sigma\epsilon_i$ ) is appropriate for evaluating the total molecular energy for a given geometry, if it is assumed that the theoretical basis of the EH method lies within the framework of minimum basis set Hartree-Fock calculations.<sup>18</sup>

Excitations were assumed for purposes of calculation to be singlet-singlet transitions between the closed-shell ground state and the excited state described by occupation of one of the virtual MO's. The excitation energy is taken as the gap between the MO's involved in the single electron jump,  $\Delta E = \epsilon_m - \epsilon_n$ , and the oscillator strength is  $f = 0.0245 \times \Delta E$  (in eV)  $\times |\mathbf{R}^{mn}|^2$ . Here  $\mathbf{R}^{mn}$  is the rigorously evaluated dipole length integral between MO's  $m$  and  $n$ . The use of a dipole velocity operator was deemed to be unwarranted at our level of treatment, although for other types of wave function this operator is preferred.<sup>19</sup> In light of earlier EH calculations on rotatory strengths,<sup>20</sup> no attempt was made to compute them here.

### Barriers to Internal Rotation

A necessary, but not sufficient, condition for proper interpretation of the uv spectra of disulfides is that the potential energy curve for internal rotation about the S-S bond be correctly described by the EH calculations. Numerous investigations<sup>12,13,21-23</sup> by other MO methods report the calculated HSSH conformation in general agreement with experiment (90° 36'),<sup>16</sup> and predict barrier heights in the ranges 2.7-9.3 kcal/mol (cis) and 0.8-6.0 kcal/mol (trans). Experimentally, the barrier heights are not yet known precisely,

(15) D. B. Boyd, *J. Amer. Chem. Soc.*, **94**, 64 (1972); D. B. Boyd in "The Purines: Theory and Experiment," E. D. Bergmann and B. Pullman, Ed., The Israel Academy of Sciences and Humanities, Jerusalem, 1972, p 48.

(16) G. Winnewisser, N. Winnewisser, and W. Gordy, *J. Chem. Phys.*, **49**, 3465 (1968).

(17) D. Sutter, H. Dreizler, and H. D. Rudolph, *Z. Naturforsch.*, **20**, 1676 (1965).

(18) D. B. Boyd, *Theor. Chim. Acta*, **20**, 273 (1971); F. P. Boer, M. D. Newton, and W. N. Lipscomb, *Proc. Nat. Acad. Sci. U. S. A.*, **52**, 890 (1964).

(19) A. J. McHugh and M. Gouterman, *Theor. Chim. Acta*, **13**, 249 (1969).

(20) R. R. Gould and R. Hoffmann, *J. Amer. Chem. Soc.*, **92**, 1813 (1970).

(21) M. E. Schwartz, *J. Chem. Phys.*, **51**, 4182 (1969).

(22) A. Veillard and J. Demuynck, *Chem. Phys. Lett.*, **4**, 476 (1970).

(23) I. H. Hillier, V. R. Saunders, and J. F. Wyatt, *Trans. Faraday Soc.*, **66**, 2665 (1970).

although present indications<sup>16,24</sup> favor values toward the upper end of the quoted ranges. Our EH calculations give the most stable conformer of HSSH a dihedral angle of 80–90° with a cis barrier of 1.5 kcal/mol and a trans barrier of 0.9 kcal/mol. Thus, even though the barrier heights seem rather low, our EH calculations give the correct shape for the potential energy curve.

In dimethyl disulfide, the experimental<sup>17</sup> CSSC dihedral angle is 85°, and the methyl groups are staggered with respect to the S–S bond.<sup>25</sup> Our EH calculations produce an equilibrium dihedral angle of about 90° and staggered methyl groups. When the methyls are staggered, the cis barrier for rotation about the S–S bond is 7.0 kcal/mol, and the trans barrier is 2.2 kcal/mol. Recent nmr evidence points to an upper limit of 7 kcal/mol for the barriers in some unsymmetrical acyclic disulfides.<sup>26</sup> When the CSSC dihedral angle is large enough to avoid steric hindrance between the methyl groups, our predicted 1.2 kcal/mol barrier to rotation about the S–C bonds is similar to the experimental<sup>17</sup> barrier of 1.6 kcal/mol. Previous calculations on the conformation of H<sub>3</sub>CSSCH<sub>3</sub> by the PCILO method<sup>27</sup> produced a preferred CSSC dihedral angle of 100°, a cis barrier of 2.9 kcal/mol, and a trans barrier of 1.3 kcal/mol. However, the methyl groups were predicted to be eclipsed at the 100° CSSC angle. Other calculations by a ZDO–SCF method<sup>14</sup> showed the total energy of H<sub>3</sub>CSSCH<sub>3</sub> to be lower at 90° than at smaller dihedral angles, but the barrier heights of 45.9 kcal/mol (cis) and 14.5 kcal/mol (trans) were abnormally high.

Mulliken<sup>28</sup> population analyses of the HSSH and H<sub>3</sub>CSSCH<sub>3</sub> wave functions, as with the *ab initio* calculations of HSSH,<sup>21–23</sup> show the largest S–S overlap population,  $n(\text{S–S})$ , is obtained at a dihedral angle of about 90°. Thus, the total energy is lowest when the S–S bond is strongest. By breaking  $n(\text{S–S})$  down to  $\sigma$  and  $\pi$  components, we obtain the interesting result that the  $\sigma$  overlap population between the sulfurs increases monotonically as the dihedral angle is opened from 0 to 180°, whereas the  $\pi$  component peaks near 90°. This means the interactions of the AO's of  $\pi$  symmetry impart the preferred 90° conformation on disulfides. A negative (antibonding) contribution is obtained from the S<sub>1</sub>3p <sub>$\pi$</sub> –S<sub>2</sub>3p <sub>$\pi$</sub>  interactions, and this contribution is least negative when the dihedral angle is 90°. The positive value for the total  $\pi$  component of  $n(\text{S–S})$  arises almost entirely from 3p <sub>$\pi$</sub> –3d <sub>$\pi$</sub>  overlaps. In fact, the 3p <sub>$\pi$</sub> –3p <sub>$\pi$</sub>  overlap population is negative with or without 3d AO's in the basis set. Thus, the strength of the S–S bond is greatest at a dihedral angle of 90° because the antibonding contributions to the  $\pi$  component of  $n(\text{S–S})$  are diminished relative to the bonding contributions from the lower filled MO's. Our interpretation of the population analysis is consistent with two qualitative arguments about the 90° preference. One<sup>29</sup> is that the barriers result from the

repulsion between the lone-pair electrons in 3p <sub>$\pi$</sub>  AO's on each sulfur. The repulsion is minimized when these AO's are orthogonal. The second argument<sup>16</sup> is based on a hyperconjugative mechanism whereby the  $\pi$  character of the S–S bond is enhanced when, for example, in HSSH, the S–H bonds are aligned for maximum transfer of electron density through the 3p <sub>$\pi$</sub>  AO's to the hydrogens as in H–S<sup>+</sup>=S H<sup>–</sup>.

Later in this paper, it will be seen that the two highest filled MO's of the disulfide moiety each have a node perpendicular to the S–S bond. Removal or polarization of electron density away from the vicinity of an orbital node between a given pair of atoms strengthens the bonding between those atoms.<sup>30</sup> This removal can be effected by introduction of a functional group whose orbitals will interact with the orbitals of the parent moiety<sup>31</sup> or by changes in conformation which enhance delocalization. Electron density maps can show the drift of electrons *via* the latter mechanism.<sup>32</sup>

### Fate of the Disulfide Chromophore under Torsion

In the preceding section satisfactory agreement between theory and experiment was achieved using the EH method. Hence we next turn to the main task of using the MO's for elucidating the dependence of the uv excitations on the conformation of the disulfide chromophore. Whereas the energies and other quantities predicted by our calculations may not agree perfectly with experiment, the examples which have been noted above and those which will be cited later in this section demonstrate that the variation with dihedral angle is indeed reproduced quite well considering we are using such a simple theory. We will begin this section by examining the nature of the MO's in the simpler disulfide HSSH. Then those MO's involved in the uv excitations of H<sub>3</sub>CSSCH<sub>3</sub> will be discussed. Energy level diagrams for HSSH and H<sub>3</sub>CSSCH<sub>3</sub> will be seen to be very similar. Hence, either would be a fairly adequate model for the disulfide chromophore. The theoretical spectra from the H<sub>3</sub>CSSCH<sub>3</sub> computations are selected for comparison with experimental data in the final part of this section. Rotation of the methyl groups about the S–C bonds in H<sub>3</sub>CSSCH<sub>3</sub> was found to have a relatively minor influence on the predicted spectra, so the numerical results will be presented for the geometry with both methyls staggered.

The energies of the filled MO's and the three lowest empty MO's of HSSH are plotted in Figure 1 as a function of dihedral angle. The character of each MO, labeled according to its symmetry with respect to C<sub>2</sub> rotation, is sketched for the cis and trans conformers. The lowest filled MO, **1a**, is essentially unaffected by conformation; it consists of a nodeless combination of the s orbitals on each center (mainly S<sub>1</sub>3s + S<sub>2</sub>3s). The next higher MO, **1b**, is the singly noded combination of the 3s AO's (S<sub>1</sub>3s – S<sub>2</sub>3s). MO **2a** is a bonding

(30) D. B. Boyd and R. Hoffmann, *J. Amer. Chem. Soc.*, **93**, 1064 (1971).

(31) An unusually small CSSC dihedral angle (66°) and short S–S bond length (2.01 Å) has been reported in dicinnamyl disulfide by J. D. Lee and M. W. R. Bryant, *Acta Crystallogr., Sect. B* **27**, 2325 (1971). The molecular conformation permits (and may be determined by) short H···S contact distances (2.3 Å) suggestive of intramolecular hydrogen bonds. The short, and therefore strong, S–S bond in this acyclic disulfide may thus be traced to the drainage of charge density away from the node separating the sulfur atoms in the high-lying MO's by the presence of these hydrogens near the lone pairs.

(32) D. B. Boyd, submitted for publication.

(24) F. Fehér and K. Seyfried, *Z. Anorg. Allg. Chem.*, **322**, 162 (1963); R. L. Redington, *J. Mol. Spectrosc.*, **9**, 469 (1962).

(25) B. Beagley and K. T. McAloon, *Trans. Faraday Soc.*, **67**, 3216 (1971).

(26) R. R. Fraser, G. Boussard, J. K. Saunders, J. B. Lambert, and C. E. Mixan, *J. Amer. Chem. Soc.*, **93**, 3822 (1971).

(27) D. Perahia and B. Pullman, *Biochem. Biophys. Res. Commun.*, **43**, 65 (1971).

(28) R. S. Mulliken, *J. Chem. Phys.*, **23**, 1833 (1955).

(29) L. Pauling, *Proc. Nat. Acad. Sci. U. S.*, **35**, 495 (1949).

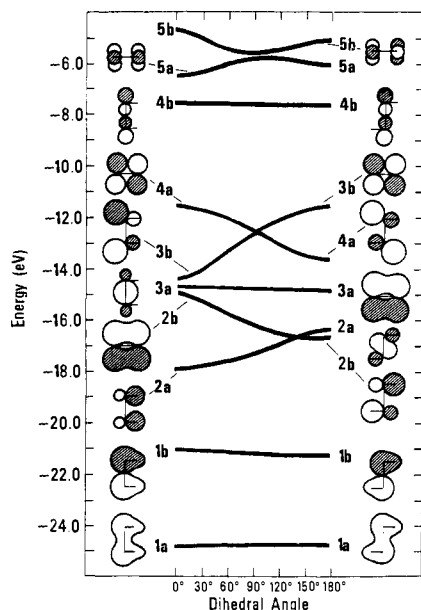


Figure 1. Correlation diagram for the variation of the MO eigenvalues ( $\epsilon_i$ ) with dihedral angle in HSSH. The shape of the MO's is depicted schematically for the  $0^\circ$  and  $180^\circ$  conformers on the left and right, respectively. The unshaded regions of each MO have the opposite sign from the shaded regions. The molecule has  $C_{2v}$  symmetry at  $0^\circ$ ,  $C_{2h}$  symmetry at  $180^\circ$ , and  $C_2$  symmetry at intermediate angles. In the ground state, each MO is doubly occupied, except **4b**, **5a**, and **5b**, which are empty.

combination of the  $3p_\pi$  AO's ( $S_13p_x + S_23p_x$ ) from 0 to about  $150^\circ$ , but beyond  $150^\circ$ , it takes on the characteristics of a S-S  $\sigma$  MO ( $S_13p_z - S_23p_z$ ; origin at  $S_1$ ). The **2b** MO also consists of a bonding combination of  $3p_\pi$  AO's ( $S_13p_y + S_23p_y$  below  $150^\circ$ , and  $S_13p_x + S_23p_x$  above  $150^\circ$ ). Contrasting with **2a** and **2b**, whose energies vary considerably with dihedral angle, is MO **3a**. At dihedral angles less than  $150^\circ$ , it is a S-S  $\sigma$  MO, but at larger angles it mixes with, and becomes at  $180^\circ$ , a  $\pi$  MO. The top two filled MO's, **3b** and **4a**, are each doubly noded and can be described as the nonbonding combinations of the  $3p_\pi$  AO's ( $S_13p_x - S_23p_x$  and  $S_13p_y - S_23p_y$  near 0 and  $180^\circ$ , or  $S_13p_x + S_23p_y$  and  $S_13p_x - S_23p_y$  near  $90^\circ$ ). These MO's are occupied by four of the so-called lone-pair electrons. Their energies vary considerably with dihedral angle and become degenerate at about  $90^\circ$ . The lowest empty MO, **4b**, has the character of a S-S  $\sigma^*$  MO with considerable admixture of the  $3d_z$  AO's ( $S_13p_z + S_13d_z + S_23p_z - S_23d_z$ ). The energy of this MO decreases very slowly with dihedral angle. MO's **5a** and **5b** depend more strongly on the dihedral angle and consist mainly of the plus and minus combinations of the  $3d_{x^2-y^2}$  AO on each center. The inclusion of the 3d AO's in the basis set has the greatest stabilizing effect on the empty MO's as expected. For instance, in the  $90^\circ$  conformer, **4b** lies at  $-0.04$  eV without 3d AO's and at  $-7.57$  eV with them. Also, inclusion of the 3d AO's results in four other low-lying virtual orbitals. In contrast, the 3d AO's only stabilize the occupied MO's **4a** and **3b** by  $\sim 0.2$  eV and even less for the other filled MO's.

A brief comparison of our correlation diagram for HSSH (Figure 1) shows that it is similar in essential features to those assumed or computed by previous workers.<sup>12,13</sup> Bergson<sup>12</sup> simply assumed the lowest

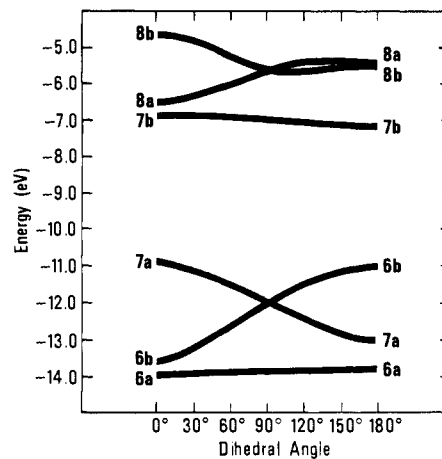


Figure 2. Correlation diagram for the variation of the MO eigenvalues ( $\epsilon_i$ ) with dihedral angle in  $H_3CSSCH_3$ . In the ground state of the molecule, MO's **6a**, **6b**, and **7a** are doubly occupied and MO's **7b**, **8a**, and **8b** are empty.

empty MO of the disulfide moiety to be more or less independent of dihedral angle and to be an antibonding S-S  $\sigma^*$  MO. Both of these assumptions are confirmed as seen in the **4b** level of Figure 1. Bergson computed the energy of the highest occupied MO to decrease and the energy of the next to the highest occupied MO to increase as the dihedral angle is opened until at  $90^\circ$  they are nearly degenerate. In Figure 1 we see that this is, indeed, the pattern of variation of **4a** and **3b**. Moreover, our calculations trace the variation beyond  $90$  to  $180^\circ$ . Depending on the hybridization assumed, Bergson placed a S-S  $\sigma$  MO third or fifth highest in energy. The EH calculations predict MO **3a**, which has S-S  $\sigma$  character in the 0 to  $90^\circ$  range, to be third highest. The CNDO calculations of Linderberg and Michl<sup>13</sup> produced an orbital description in fair accord with ours. The lowest empty MO was a S-S  $\sigma^*$  orbital. The two highest occupied MO's were similar to **3b** and **4a** with most of the parameter sets tried, although for some parameters their S-S  $\sigma$  MO was highest in energy. The crossover between their MO's corresponding to **3b** and **4a** occurred at dihedral angles between  $70$  and  $90^\circ$  depending on the parameters.

The three highest filled MO's and the three lowest empty MO's of  $H_3CSSCH_3$  are predicted to be appropriately spaced for absorption of uv radiation. The variation of these energy levels, labeled according to their symmetry in the  $C_2$  point group, is plotted in Figure 2. The principal forms of these MO's are not unlike those for HSSH. The energy of MO **6a** varies only slightly with dihedral angle because this MO has S-S  $\sigma$  bonding character from 0 to about  $150^\circ$ . Similar to the case of HSSH, **6a** takes on  $\pi$ -type ( $S_13p_y + S_23p_y$ ) character beyond  $150^\circ$ . Highly dependent on dihedral angle are the lone-pair MO's **6b** and **7a**. These are nearly degenerate at  $90^\circ$  and cross at a few degrees above  $90^\circ$ . They are the nonbonding combinations of the  $3p_\pi$  AO's on each sulfur. The lowest empty MO **7b** is of S-S  $\sigma^*$  character and becomes less unstable as the dihedral angle is opened. The 3d AO's enter **7b**, and also **8a** and **8b**, quite heavily.

Previous semiempirical calculations on the MO's of  $H_3CSSCH_3$  by Cusachs' EH method<sup>6</sup> resulted in considerable disparity between theory and experiment.

Although the qualitative nature of their three highest filled MO's appears to be not unlike ours, all the low virtual orbitals lay too close to the filled MO's, giving rise to vertical excitations as low as 2.1 eV ( $\sim 590$  nm). Thompson, *et al.*,<sup>6</sup> were led to the conclusion that the 250 nm band in dimethyl disulfide arose from excitations from an MO with S3p character to two virtual MO's, one being S-S  $\sigma^*$  and the other being S4s. This explanation coincided with their discovery that the 250 nm band could be partially resolved into two overlapping transitions.<sup>6</sup> However, two transitions would also be expected at  $90^\circ$  because **7a** and **6b** are nearly degenerate as seen in Figure 2. Hence the existence of two transitions in the 250 nm band can be explained by the presence of only one virtual MO (the S-S  $\sigma^*$ , **7b**) and two filled MO's (**7a** and **6b**). Linderberg and Michl<sup>13</sup> have also noted that the first absorption band in both  $\text{H}_3\text{CSSCH}_3$  and  $\text{HSSH}^{33}$  is very broad and capable of accommodating two nearly degenerate transitions. A correlation diagram for  $\text{H}_3\text{CSSCH}_3$ , which is similar to ours, has been published by Yamabe, *et al.*, for the  $0$  to  $90^\circ$  range of dihedral angles.<sup>14</sup>

Transition energies and oscillator strengths for  $\text{H}_3\text{CSSCH}_3$  were computed for all possible one-electron excitations involving the MO's of Figure 2. The predicted spectra at various CSSC dihedral angles are plotted in Figure 3. In Table II are the computed

**Table II.** Computed  $\lambda_{\text{max}}$  (nm) and Oscillator Strengths for Some Excitations in  $\text{H}_3\text{CSSCH}_3^a$

Dihedral angle, deg	<b>7a</b> $\rightarrow$ <b>7b</b>		<b>6b</b> $\rightarrow$ <b>7b</b>		<b>6a</b> $\rightarrow$ <b>7b</b>	
	$\lambda_{\text{max}}$	$f$	$\lambda_{\text{max}}$	$f$	$\lambda_{\text{max}}$	$f$
0	306	0.02	183	0.12	174	0.75
30	291	0.05	196	0.07	175	0.71
60	268	0.11	218	0.04	178	0.62
90	247	0.20	245	0.03	181	0.50
120	228	0.35	277	0.015	183	0.35
150	216	0.55	307	0.007	184	0.13
180	211	0.67	319	0.005	184	0.0

<sup>a</sup> Of the numerous notations which have appeared in the literature for the first two transitions of the disulfide chromophore, we advocate the generic designations  $n_a \rightarrow \sigma^*$  and  $n_b \rightarrow \sigma^*$ . The **6a**  $\rightarrow$  **7b** excitation may be designated  $\sigma \rightarrow \sigma^*$  for dihedral angles relevant to experiment.

data for excitations to MO **7b**. The longest wavelength line is seen to vary with dihedral angle in a manner consistent with experiment (Table I). At  $0^\circ$  this so-called first transition is computed at a long wavelength of 306 nm ( $f = 0.02$ ). The transition blue-shifts and intensifies until at  $90^\circ$  it comes at 247 nm ( $f = 0.20$ ). Through this range of dihedral angles the excitation is from the lone-pair type MO **7a** to the S-S  $\sigma^*$  MO **7b**. Beyond  $90^\circ$ , it is **6b**  $\rightarrow$  **7b**. The intensity therefore becomes very weak and red-shifts as the dihedral angle is opened to  $180^\circ$ . At  $180^\circ$ , the first transition comes at 319 nm ( $f = 0.005$ ). Although the experimental trends are reproduced by our EH method, the gap between the highest occupied and lowest empty MO's is too large at small dihedral angles. Since MO **7b** varies little with conformation, MO **7a** should be at higher energies at small dihedral

(33) F. Fehér and H. Münzner, *Chem Ber.*, **96**, 1131 (1963).

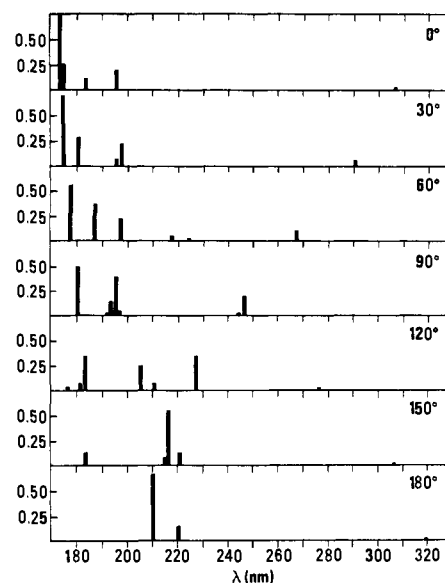


**Figure 3.** Computed electronic spectra of  $\text{H}_3\text{CSSCH}_3$  at the indicated dihedral angles. Intensities of the transitions are represented by the oscillator strengths,  $f$ , plotted vertically. Atomic coordinates ( $x, y, z$  in Å) are  $S_1$  at 0, 0, 0;  $S_2$  at 0, 0, 2.038;  $C_3$  at 1.765, 0, 2.439; and  $C_4$  at 1.765, 0,  $-0.401$  at  $0^\circ$ , 0,  $-1.765$ ,  $-0.401$  at  $90^\circ$ , and  $-1.765$ , 0,  $-0.401$  at  $180^\circ$ . With respect to this coordinate system, the components ( $x, y, z$  in au) of the transition moment integrals,  $R^{mn}$ , for the **7a**  $\rightarrow$  **7b** transition are 0,  $-0.48$ , 0 at  $0^\circ$ ,  $-0.32$ ,  $-0.32$ ,  $-1.19$  at  $90^\circ$ , and  $-0.63$ , 0,  $-2.07$  at  $180^\circ$ . The **7a**  $\rightarrow$  **7b** transition is polarized in a plane perpendicular to the  $C_2$  rotation axis with angles of  $90$ ,  $46.5$ ,  $29$ ,  $21$ ,  $18$ ,  $17.3$ , and  $17^\circ$  between the  $R^{mn}$  and S-S vectors at the tabulated dihedral angles. The **6b**  $\rightarrow$  **7b** transition is always polarized parallel to the  $C_2$  axis.

angles for the virtual orbital approximation to work well here.<sup>34</sup> The higher bands of the disulfide chromophore are subject to the effects of configuration interaction to a greater extent than is the first transition.<sup>13</sup> However, the trends in the conformational dependence of these higher bands as seen in Figure 3 may be of some significance. It is conceivable that with a more sophisticated calculational procedure additional low-lying excited states, and hence additional transitions between the S-S  $n_a \rightarrow \sigma^*$ ,  $n_b \rightarrow \sigma^*$ , and  $\sigma \rightarrow \sigma^*$  bands, would be predicted. In the remainder of this paper, the predicted spectra will be related to experimental data for assorted disulfide compounds which have dihedral angles between  $120$  and  $60^\circ$ .

The recent CD study<sup>8</sup> on [2,7-cystine]-gramicidin S assigned transitions at 272 nm and 230 nm to the disulfide chromophore. They estimated the dihedral angle to be about  $120^\circ$ . Reading from Table II and Figure 3, we would predict transitions to occur at 277 nm ( $f = 0.015$ ) and 228 nm ( $f = 0.35$ ) for a dihedral angle of  $120^\circ$ . The agreement between theory and experiment is thus astonishingly good in this example.

(34) Another factor in the case of acetylarnotin (Table I) may be that dimethyl disulfide is not an adequate model because of the perturbing effect of the piperazinedione ring. A perturbation of the electronic structure of the disulfide moiety can be inferred from X-ray crystallographic studies (see ref 3; J. Fridrichsons and A. M. Mathieson, *Acta Crystallogr.*, **23**, 439 (1967); M. O. Chaney and N. D. Jones, unpublished work). In crystalline epidithiadiketopiperazine systems, the twist of the disulfide group is usually such that each sulfur is displaced toward the proximal carbonyl carbon rather than toward the proximal ring nitrogen. Hence there may be an electrostatic attraction between the sulfur lone-pair electrons and the positively charged<sup>10</sup> carbonyl carbons. This attraction would perturb the high-lying MO's involved in the disulfide chromophore.

Several investigators<sup>1,35</sup> have pointed out that the absorption maximum of dialkyl disulfides is displaced to progressively shorter wavelengths in the series: dimethyl (255 nm), diethyl (252 nm), diisopropyl (245 nm), and di-*tert*-butyl (230 nm by extrapolation). One factor determining these shifts may be that the increasing bulk of the alkyl group opens the CSSC dihedral angle beyond 90°. <sup>36</sup> The **6b** → **7b** transition would be the first transition in this range, but as mentioned above, it is very weak (*e.g.*,  $f = 0.015$  at 120°). Hence possibly this transition is not being detected, and instead the **7a** → **7b** line is. This transition is 7–20 times more intense between 90 and 120° than is **6b** → **7b**. Thus, the absorption maxima reported for dialkyl disulfides at wavelengths shorter than ~250 nm may, in fact, be due to the second transition and not the first.

In cystine, where the dihedral angle is about 90°, there is, in addition to the 250 nm band mentioned above, another optically active transition at 186 nm.<sup>37</sup> From Figure 3, it is seen that we compute the first and second transitions to be almost degenerate at about 245–247 nm. The 186 nm transition could be assigned to the four probably unresolvably close lines around 195 nm due to excitations into the 3d MO's,

(35) N. A. Rosenthal and G. Oster (*J. Amer. Chem. Soc.*, **83**, 4445 (1961)) explain the hypsochromic shift of  $\lambda_{\max}$  in dialkyl disulfides, RSSR, on the sole basis of hyperconjugative transfer of charge to the sulfurs because RSeSeR compounds show a similar effect. Actually, Se–Se bonds are only ~0.3 Å longer than S–S bonds. But some delocalization effect may widen the gap between  $n_a$  (or  $n_b$ ) and  $\sigma^*$  as the number of carbons in R increases up to a certain point. Methylation of HSSH does increase this gap (Figure 1 vs. Figure 2). The large shifts observed with bulkier R groups (especially *tert*-butyl) are more likely linked to changing CSSC dihedral angle. Moreover, the  $\epsilon_{\max}$  values parallel the  $f$  values predicted for the **7a** → **7b** transition as a function of dihedral angle.

(36) H. Bock and G. Wagner, *Angew. Chem., Int. Ed. Engl.*, **11**, 150 (1972), estimate the CSSC dihedral angle to be about 110° in di-*tert*-butyl disulfide. The photoelectron ionization potentials (IP) reported in this paper for RSSR compounds can be interpreted to support the crossing of the highest two occupied MO's,  $n_a$  and  $n_b$ , as the dihedral angle is opened from ~60 to ~110°. But for RSSR all with a dihedral angle about 90°, the IP's appear to depend mainly on a delocalization effect, whereby increasing the number of carbons in R decreases the gap between  $n_a$ ,  $n_b$ , and the continuum. See also R. F. Hudson and F. Filippini, *J. Chem. Soc., Chem. Commun.*, 726 (1972).

(37) D. L. Coleman and E. R. Blout, *J. Amer. Chem. Soc.*, **90**, 2405 (1968).

or, more likely, to the line at 181 nm, arising from the **6a** → **7b** transition.

Another compound with a CSSC dihedral angle near 90° is dimethyl disulfide in its equilibrium conformation. The experimental vapor spectrum<sup>6</sup> consists of a broad low maximum at 250 nm ( $f = 0.031$ ), a shoulder at about 210 nm ( $f = 0.028$ ), and a peak at 196 nm ( $f = 0.303$ ). As mentioned before we believe the broad 250 nm band to arise from the nearly degenerate excitations **7a** → **7b** and **6b** → **7b**, which we compute at 247 and 245 nm, respectively. The shoulder at 210 nm could be related to the group of lines around 195 nm associated with excitations into the empty 3d orbitals, **8a** and **8b**. The observed peak at 196 nm is very intense relative to the two shorter wavelength bands. This could coincide with the fact that the computed 181 nm band (**6a** → **7b**) has an oscillator strength (0.50) much greater than the other two bands (Table II and Figure 3). Obviously, quantitative agreement between the theoretical and experimental  $\lambda_{\max}$  and  $f$  values is not as great as one would desire, but, nevertheless, the agreement is close enough to indicate the feasibility of the assignments.

In 1,2-dithianes where the CSSC dihedral angle is approximately 60°, the first band is observed<sup>5,38</sup> in the range 280–290 nm with  $\epsilon$  300–400, and the second band is seen at 240 nm with  $\epsilon$  150–200. Examining Table II and Figure 3, the first transition (**7a** → **7b**) is at 268 nm ( $f = 0.11$ ). At shorter wavelengths there are predicted to be two weak transitions, the stronger being **6a** → **7b** at 218 nm ( $f = 0.04$ ) and the other involving 3d orbitals. Thus, both the first and second transitions can be associated with predicted lines (within ~20 nm), and the relative intensities of the first and second transitions are correctly predicted.

**Acknowledgment.** The author has benefited from helpful discussions with M. M. Marsh and L. A. Neubert.

(38) J. P. Casey and R. B. Martin (*ibid.*, **94**, 6141 (1972)) report CD and uv data for *trans*-2,3-dithiadecalin. Besides the 290- and 240-nm bands, they also observe a very strong ( $\epsilon$  4000–5000) transition at ~200 nm. Calculations on the 60° model (Figure 3) predict three highly allowed transitions at or slightly below this wavelength: a very strong  $\sigma \rightarrow \sigma^*$  band (Table II), plus two other strong transitions involving the 3d orbitals.